DIVERSITY IN CARBON K-EDGE XANES AMONG PRESOLAR GRAPHITE GRAINS. E. Groopman[1], L. R. Nittler[2], T. J. Bernatowicz[1] ,T. K. Croat[1], E. Zinner[1], A. L. D. Kilcoyne[3], [1]Laboratory for Space Sciences, Washington University in St. Louis, MO 63130, USA [2]Dept. of Terrestrial Magnetism, Carnegie Institution of Washington, Washington, DC 20015, USA [3]Advanced Light Source, Lawrence-Berkeley National Laboratory, Berkeley, CA 94704, USA (eegroopm@physics.wustl.edu).

Introduction: We report on X-ray absorption near-edge structure (XANES) measurements of 13 presolar graphite grains. High-density (HD) and low-density (LD) graphite grains from the Murchison and Orgueil meteorites were studied in the NanoSIMS and subsequently ultramicrotomed into 70nm-thick sections, which were deposited on holey-C and SiO coated TEM grids [1,2]. The LD grains likely originated in Type-II supernovae (SNe), while the HD grains likely formed in aymsptotic giant branch (AGB) stars, based upon their isotopic compositions [3].

Experimental Methods: C K-edge XANES spectra were acquired at Beamline 5.3.2 of the Advanced Light Source at Lawrence-Berkeley National Laboratory. A full description of the instrument is presented in [4]. An interferometer-controlled piezoelectric stage allows for fine-scale x,y rastering of the sample relative to the ~40nm stationary soft X-ray beam. By stepping up the monochromated beam energy after each raster, in increments as small as 0.1 eV, one can generate a data "stack", a 3-dimensional image in x × y × eV, where each raster point contains a full energy spectrum. Raster areas are set up so that they contain regions with holes in the sample to record the baseline intensity, I_0. Absorbance, or the optical density (OD) of the sample, is calculated as OD = -log(I/I_0), where I is the measured intensity through the sample. Reported energies were calibrated using CO_2 gas.

A linear pre-edge fit (270-282 eV) was subtracted from each spectrum. The major aromatic π^* peaks were fitted to an asymmetric Lorentzian profile of the form:

$$L_{asym.}(x) = \frac{\pi \cdot Aw/\left(1 + e^{-a\cdot(x-x_0)}\right)}{(x-x_0)^2 + w^2/(1+e^{-a\cdot(x-x_0)})^2}$$

where A is the amplitude, x_0 is the median (center) energy, a is an asymmetry factor, and w is the full width at half-maximum (FWHM) [5]. w was allowed to vary sigmoidally, $w \rightarrow 2\cdot w/[1 + \exp(-a\cdot(x-x_0))]$, which models peak tails very well. Note that when a = 0, w returns to its symmetric Lorentzian form, but when $a \neq 0$, the peak maximum, p, is no longer equal to x_0. We calculated the mean peak energy, μ:

$$\mu = \frac{\int_{x_0-5w}^{x_0+5w} x \cdot \mathrm{OD(x)}}{\int_{x_0-5w}^{x_0+5w} \mathrm{OD(x)}}$$

where the limits of integration were set widely enough to encompass the entire absorption peak. The standard method for deconvolving peaks in a XANES spectrum is to model the various ionization edges as arctangent or step functions and subtract these from the spectrum before fitting peaks [6]. This requires assumptions regarding which edges are present in addition to their exact locations and intensities. Here we report quantitative results only for the aromatic π^* absorptions, which are at lower energies than the aromatic ionization edge (~290.5 eV) and other ionization edges, and so are not affected by the exclusion of ionization edge subtraction. While the π^* resonances are sensitive to the orientation of the aromatic sheets relative to the beam, this should only affect the peak's amplitude and not its FWHM [7]. All spectra in the figures are normalized to the area under the σ^* peaks between 291 and 293 eV.

Sample	FWHM *w* (eV)	Median x_0 (eV)	Peak *p* (eV)	*Mean* μ *(eV)*	*a*
KE3-e6C	2.47	285.55	285.3	285.43	-0.93
OR1d5m-11	1.08	285.28	285.3	285.27	0.03
OR1d5m-15	5.83	286.16	285.3	285.55	-0.80
OR1d5m-20	1.13	285.37	285.3	285.31	-0.93
OR1d5m-24	2.76	285.52	285.2	285.40	-0.99
OR1d6m-6 Core	4.85	285.93	285.3	285.50	-1.47
OR1d6m-6 Mantle	4.40	285.81	285.2	285.49	-1.65
OR1d6m-13	1.89	285.51	285.3	285.51	-0.89
OR1d6m-17	1.51	285.41	285.3	285.50	-0.62
OR1d6m-18[1]	1.78	285.40	285.2	285.45	-0.94
OR1d6m-18[2]	1.51	285.36	285.2	285.43	-1.06
OR1d6m-23	1.87	285.27	285.1	285.23	-0.89
OR1d6m-24	2.25	285.54	285.3	285.52	-1.01
OR1f3m-38	1.33	285.06	285.0	285.08	-0.45
OR1g2m-4	2.29	285.58	285.3	285.44	-0.86

Table 1: Murchison graphite grain: KE3 (ρ = 1.6-2.05 g/cm^3). Orgueil graphite grains: OR1d (ρ = 1.75-1.92 g/cm^3), OR1f (ρ = 2.02-2.04 g/cm^3), OR1g (ρ = 2.04-2.12 g/cm^3), e.g. 6m = 6th mount [1,2]. Two microtome sections from OR1d6m-18 exhibited variation in their spectra. All other grains showed consistent spectra across multiple sections.

Results: XANES spectra from pure terrestrial graphite are characterized by strong aromatic π^* (285.2 eV) and σ^* (291.5 & 292.5 eV) excitons from C(1s) transitions [7]. All of the presolar grains exhibit graphite-like spectra. The spectra of many of the grains also contain minor peaks corresponding to aliphatic (287.3–288.1 eV), ketone (286.5 eV), and carboxyl (288.4–288.7 eV) absorptions [8,9]. Each grain spectrum con-

tains a different combination of minor absorptions. Six grains show aliphatic resonances; two grains ketone resonances; and nine grains carboxyl resonances. The HD grain OR1f3m-38 has a spectrum that is recognizably graphitic, however its π^* peak energy is 285.0 eV, lower than that of terrestrial graphite, and its σ^* absorptions are much broader than in any other graphite grains. As HD graphite grains typically contain less-disrupted graphite than their LD turbostratic cousins [10], it is interesting that the spectrum of one of the two HD grains in this study contains multiple minor organic peaks and looks the least like pure graphite.

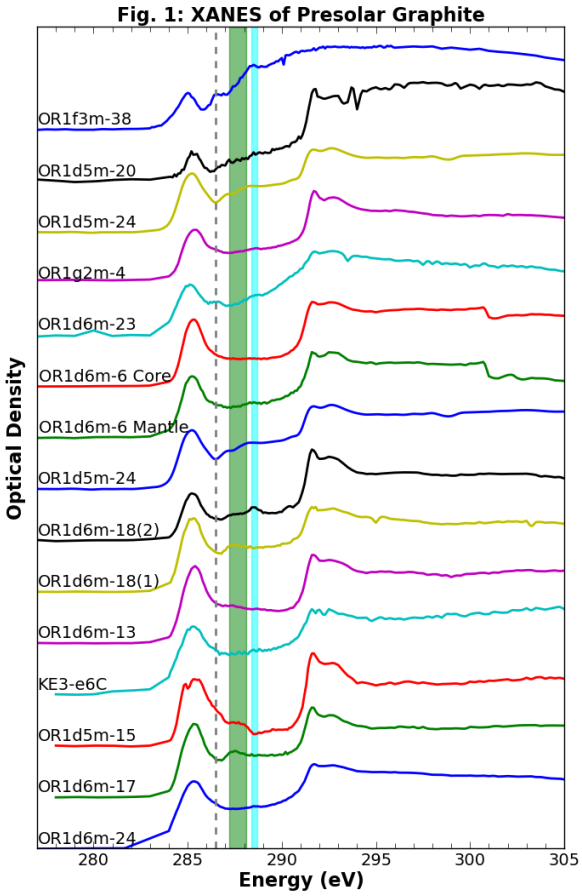

Figure 1: Presolar graphite XANES spectra exhibiting mostly graphite-like features. Many minor peaks are also present: ketone (dashed, 286.5 eV), aliphatic (green, 287.3–288.1 eV), and carboxyl (cyan, 288.4–288.7 eV), with composition varying from grain to grain.

The peak energies of the aromatic π^* absorptions range from 285.0 to 285.4 eV, with the majority of grains at 285.2 and 285.3 eV (see Table 1). The FWHM range from 1.1 to 5.8 eV, which, in conjunction with varying degrees of asymmetry, yield mean energies from 285.1 to 285.6 eV. One grain, OR1d6m-6, contains a nanocrystalline core surrounded by a mantle of turbostratic graphite [11]. Peak fit parameters for both regions are given in Table 1. The nanocrystalline core spectrum perfectly matches that of aromatic carbon, which reflects its composition of 2-4nm sheets of graphene, determined by electron diffraction studies (Fig. 2). The turbostratic graphite spectrum contains a small carboxyl peak (288.4 eV) and a longer tail on its $\boldsymbol{\pi^*}$ resonance. These likely reflect the enhanced O content characteristic of turbostratic graphite vis-à-vis pure graphite.

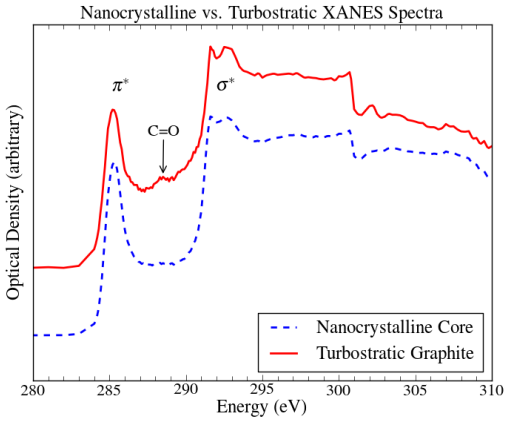

Figure 2: Comparison of XANES spectra from nanocrystalline core and turbostratic mantle or OR1d6m-6 [11]. The nanocrystalline core exhibits a perfect aromatic spectrum, reflecting its composition of 2-4nm sheets of graphene. The mantle contains a small carboxyl peak.

Discussion: The diversity in the variety and abundance of minor organic peaks within the XANES spectra may reflect the varied formation conditions of the presolar graphite grains. All grains exhibit graphite-like spectra, which agree well with TEM observations. The majority of grains in this study (11) originated in SNe and contain excesses in ^{18}O relative to terrestrial/the sun. Minor peaks from O-containing compounds in these grains are therefore most likely indigenous and not due to contamination. Future quantitative analyses of these minor peaks will help to shed more light on the chemical compositions and origins of these grains.

References: [1] Croat, T.K. et al. (2003) *GCA* 67:4705-4725 [2] Groopman, E. et al. (2012) *ApJL* 754:L8. [3] Zinner, E. (2013) *Treatise on Geochemistry, 2nd ed.* 1.4:181-213 [4] Kilcoyne, A.L.D (2003) *J. Synchrotron Rad.* 10:125-136 [5] Stancik & Brauns (2008) *Vibrational Spectroscopy* 47:66-69 [6] Cody, G. et al. (1995) *Energy & Fuels* 9:75-83 [7] Brandes, J.A. et al. (2008) *Carbon* 46:1424-1434 [8] Cody , G. et al. (2008) *Meteorit. Planet. Sci* 43:353-365 [9] DeGregorio, B.T. et al. (2013) *Meteorit. Planet. Sci* 48:904-928 [10] Croat, T.K. et al. (2008) *Meteorit. Planet. Sci* 43:1497-1516 [11] Groopman, E. et al. (2013) *Meteorit. Planet. Sci* 48: abs. #5072